24p

NASA TM X- >0 680

MAGNETIC FIELD OBSERVATIONS NEAR MERCURY: PRELIMINARY RESULTS FROM MARINER 10

N. F. NESS

K. W. BEHANNON

R. P. LEPPING

Y. C. WHANG

K. H. SCHATTEN

MAY 1974

GSFC —— GODDARD SPACE FLIGHT CENTER ——

GREENBELT, MARYLAND

MAGNETIC FIELD OBSERVATIONS NEAR MERCURY:

PRELIMINARY RESULTS FROM MARINER 10

ABSTRACT

Results are presented from a preliminary analysis of data obtained near Mercury on 29 March 1974 by the NASA/GSFC Magnetic Field Experiment on Mariner 10. Rather unexpectedly, a very well developed, detached bow shock wave, which develops as the super-Alfvenic solar wind interacts with the planet, has been observed. In addition, a magnetosphere-like region, with maximum field strength of 98γ at closest approach (704 km altitude), has been observed contained within boundaries similar to the terrestrial magnetopause. The obstacle deflecting the solar wind flow is global in size, but the origin of the enhanced magnetic field is not yet uniquely established. It may be intrinsic to the planet and distorted by interaction with the solar wind. It may also be associated with a complex induction process whereby the planetary interior-atmosphere-ionosphere interacts with the solar wind flow to generate, by a dynamo action, the observed field. The most plausible explanation, considering the complete body of data, favors the preliminary conclusion that Mercury has an intrinsic magnetic field. If correct, this would represent a major scientific discovery in planetary magnetism and have considerable impact on studies of the origin of the solar system.

INTRODUCTION

Results from a preliminary analysis of quick-look data obtained by the NASA/GSFC Magnetic Field Experiment during Mercury encounter on 29 March 1974 are summarized in this report. The purpose of this investigation was to study the magnetic field environment of the planet Mercury and the nature of the solar wind interaction with it. There is substantial evidence in this initial assessment of the results to support the preliminary conclusion that an intrinsic planetary magnetic field exists. Rather unexpectedly, a very well developed, strong and detached bow shock wave was observed as well as a magnetosphere-like region in which the field magnitude increased to 98γ at closest approach, 704 km from the planetary surface. This is a factor of 5 greater than the average interplanetary magnetic field strength of 18γ measured outside the Hermean bow shock.

Scientific interest in Mercury received a major stimulus in 1965 from data provided by radar observations of the planet. It was discovered (1) that the planet's rate of rotation was not synchronous with its orbital motion. Explanations for this remarkable result were soon forthcoming (2), and a new era in planetary studies began in which coupling of orbital motion and rotation rates was found to be considerably more complex and informative than previously expected.

For some time, it has been acknowledged that Mercury is quite anomalous among the terrestrial planets with a remarkably high average density of 5.6 gm/cm^3 for its small radius of 2434 km (3). Studies of the planet's interior have been hampered both by the inadequacy of available data concerning its shape, size and mass as well as by the absence of

definitive information concerning its rotational axis and precessional motion. Only recently have attempts been made to study these problems and their significance in the history of the formation of Mercury (4).

The atmosphere of Mercury has also been the subject of considerable speculation (5), the earlier work being prejudiced by the erroneous assumption of synchronous rotational-orbital periods. Studies incorporating the new radar results (6) suggested that revisions of the traditional concept of a planet devoid of an atmosphere was necessary.

In the absence of any evidence for appreciable rotation of the planet or for a substantial atmosphere, it was thought that the planet Mercury would resemble our own Moon in many respects. Taking into account recent observations of microwave emissions and the newly established correct rotation period for the planet, it was suggested strongly that surface thermo-physical characteristics of the planet would be rather close to those of the Moon (7). There was no evidence for any radio emissions from the planet Mercury such as those from Jupiter's radiation belts.

Thus with the traditional view of geomagneticians that a rapidly rotating planet with some precession were features essential for generation of a planetary magnetic field (8), there was little reason to suggest an intrinsic field of Mercury. There were some very elementary estimates of a planetary magnetic field made on very simple scaling laws of planetary volumes and/or rotation rates, but the bases for these studies were rather speculative.

Specific studies related to the solar wind interaction with Mercury depended upon its physical characteristics. Figure 1 summarizes four

modes of interaction, of which three have been observed in the exploration of the solar system. In Model A, a lunar type interaction was proposed (9), based upon an atmosphere-ionosphere insufficient to deflect the solar wind flow and planetary interior with electrical conductivity insufficient for induction of a significant secondary magnetic field. In Model B, a modest atmosphere-ionosphere was proposed (10) and a deflected solar wind flow anticipated, contingent upon the specific model of the atmosphere assumed. In this model there was no discussion of the magnetic field in the vicinity of the planet associated with the complex interaction with the magnetized solar wind.

Basic concepts of the induction of a secondary magnetic field were developed in association with studies of the solar wind interaction with the Moon (11). Either a steady state field could be induced due to the convective flow of the magnetized solar wind past the planet or a transient field associated with changes in the interplanetary magnetic field as observed at the planet. In the case of the Moon, the low electrical conductivity of the surface layer decouples the planet from the solar wind for the steady state interaction mode and only the transient mode of induction is significant. Model C depicts, very qualitatively, a steady state induction mode with the question marks indicating regions where critical uncertainties exist regarding the interaction process and magnetic field topology.

Most authors conditioned their studies on the assumption that Mercury did not possess a sufficiently significant magnetic field for deflection of solar wind flow. However, for completeness of this discussion and because of the results obtained, we include the solar

wind interaction with the earth's magnetic field, model D. Here a substantial magnetosphere is developed which contains permanently trapped energetic particles forming the radiation belts and includes a very well developed, large magnetic tail extending far downstream away from the Sun, much like a comet tail.

INSTRUMENTATION

The magnetic field experiment consists of two triaxial fluxgate magnetometers. The dual magnetometer system used on Mariner 10 and its performance characteristics have already been described in the Venus encounter results (12). During Mercury encounter, the instrument operated continuously in the high range with each axis covering $\pm 128\gamma$. Vector measurements at intervals of 40 msec with 10 bit precision yielded quantization step sizes of 0.26γ. The root mean square noise level of each sensor over the 0 to 12.5 Hz band pass ranged between 0.03 and 0.06γ, significantly less than the digitization value.

We shall not discuss the instrument further except to remark that as the spacecraft passed through solar occultation at Mercury, no significant change in the spacecraft magnetic field was noted. This provides experimental in-flight verification of the assumption that the magnetic field of the spacecraft solar array panels was negligible. This solar array feature was designed by appropriate backwiring and tested pre-flight but was not checked at Venus encounter since no solar occultation occurred there. During Mercury encounter, a variable space-craft magnetic field was observed with a maximum of 4γ at the outboard magnetometer.

At this early date, the accuracy of the measurements, combining

all sources of error, is estimated to be approximately $\pm 1\gamma$ on each axis. The nature of the results and the magnitude of the fields measured is such that this is not a source of significant error in this preliminary report.

MERCURY ENCOUNTER OBSERVATIONS

The trajectory of Mariner 10 during Mercury encounter was uniquely well positioned to study the planetary magnetic field and solar wind interaction. The spacecraft passed approximately perpendicular to the planet-Sun line on the darkside of the planet, very close to the anti-solar point. See Figure 2 for a presentation of the trajectory in Mercury centered solar ecliptic (SE) coordinates. As is readily evident, the spacecraft moved rapidly past the planet, the relative velocity being 11 km/sec. Thus, accurate information relating the time of data acquisition to the time of relative position of Mariner 10 to the planet is very important.

Magnetic field observations during a two hour time interval surrounding closest approach are shown in Figure 3. The format for presentation incorporates 6 second averaging periods for each orthogonal component of the magnetic field and a reconstituted average vector represented by a field intensity $\bar{F}$ at latitude θ and longitude ϕ in SE coordinates. The RMS parameter, which is coordinate system invariant, is sensitive to fluctuations on the time scale of 10's of seconds or less.

Shortly after closest approach, the spacecraft passed into a period of radio occultation during which data were stored on a spacecraft magnetic tape recorder for subsequent retransmission. Special processing at

Jet Propulsion Laboratory, Pasadena, California has made available to
us quick-look data tapes for both the real time data as
well as the play-back data at encounter.

As Mariner 10 approached the planet, the interplanetary magnetic
field was slightly disturbed, relative to observations performed several
days previous, as measured by the RMS value and as noted in the variable
average field magnitude and direction. The magnitude was $18 \pm 2\gamma$,
only slightly lower than expected when extrapolating the average magnetic
field of 6γ observed at 1 A.U. to the Mercury encounter heliocentric
distance of 0.46 A.U. The well known formulae for the Archimedian
spiral magnetic field imbedded in the interplanetary medium would
predict a field magnitude of 22γ at a solar azimuthal angle $\emptyset$ of 155°
or 335° for a 400 km/sec solar wind.

As can be seen from the data in this figure, there are significant,
discontinuous changes of the magnetic field in the vicinity of the planet
Mercury. These cannot be interpreted in terms of a variable interplanetary
magnetic field being swept past the spacecraft. The figure includes
identification of both inbound and outbound bow shock crossings as well
as apparent magnetopause traversals. The interpretation of these
phenomena is based on our understanding of the bow shock and magnetopause
observed in the terrestrial case. The character of the magnetic field
observations is immediately reminiscent of observations obtained
with a spacecraft traversing the earth's magnetosphere on the darkside
at a distance of approximately 8-12 earth radii.

The very sharp change in magnetic field strength to values greater
than 40γ noted at 2027-28 UT represents the inbound crossing of the

Hermean bow shock. In fact, there were three crossings which occurred during this time interval. The jump characteristics of the magnetic field at the bow shock will be discussed later in connection with a presentation of the more detailed data. Subsequently, the spacecraft is immersed in a sheath or boundary layer in which a disturbed magnetic field regime exists. As the spacecraft continues along the trajectory, the field magnitude decreases steadily to 30γ in a manner characteristic of a steady state magnetosheath. Mariner 10 again traverses a sharp boundary at 2037 UT at which the magnitude of the field increases to greater than 40γ, while the fluctuations decrease significantly. Most importantly, the direction of the magnetic field simultaneously changes abruptly by 135° (See $\emptyset$ plot in Figure 3). The magnetic field then increases steadily up to the maximum of 98γ near closest approach at 2047 UT. The direction of the magnetic field is mainly parallel to the Mercury-Sun line with a polarity sense away from the planet. There is also a smooth but small variation in the orientation of the field throughout this time period.

Following closest approach, there occurred a distinct change in the character of the magnetic field. Large amplitude variations over a wide range of time scale are observed. A large field depression with a minimum of 17γ occurs precipitously just after closest approach, with the field magnitude rising back soon afterwards to 70γ. Subsequently, the field magnitude is considerably variable while at the same time the direction has steadily changed, and is now pointing northward relative to the ecliptic. The considerable variability in the field magnitude is not accompanied by a comparable variability in field direction.

During 2054-2055 UT, the magnetopause is crossed outbound, although it is a less distinct crossing and the field directional change is primarily a change from northward to southward. As the spacecraft continues on in the sheath, it encounters magnetic fields highly variable in both direction and magnitude and the bow shock crossing is not readily apparent in this format.

Based upon the detailed 40 msec data, to be presented shortly, the outbound bow shock crossing (or crossings) occurred somewhere during 2057-2059 UT within the region indicated in Figure 3. This bow shock crossing is similar to that observed by Mariner 10 during Venus encounter (12) in which there was no abrupt and distinctive jump. This is probably associated with the relative geometry of the upstream interplanetary magnetic field and the shock surface. When the interplanetary field direction is closely aligned with the shock surface normal, it is referred to as a parallel shock. Under such circumstances, large amplitude fluctuations are known to occur from studies of the earth's bow shock (13). This type of pulsation bow shock occurs moderately often on the dawn side of the earth's bow shock because of the Archimedean spiral geometry of the interplanetary magnetic field.

More detailed presentations of subsets of the data are given in Figures 4 and 5. In addition to F, θ and ∅ describing the instantaneous vector measurements at 40 msec intervals, the XYZ SE components are also presented. The clear and distinctive appearance of high frequency fluctuations just outside the inbound bow shock is evident in Figure 4, left panel. That three crossings occurred is interpreted as representing relative motion of the bow shock across the spacecraft due to moderate changes

in the upstream interplanetary medium and the response of the Hermean
bow shock configuration. The nature of the fluctuations in the sheath
region is seen to be rather different. High frequencies are observed
outside, i.e., upstream from the bow shock while relatively lower
frequencies are observed in the sheath, i.e., downstream.

Inside the magnetopause, the field is seen to be very steady and any
fluctuations are very small. This character of the magnetic field
is continued through to the maximum field period shown in the right most
panel. Small sinusoidal perturbations of the magnetic field, analogous
to micropulsations observed terrestrially, are observed between 2045-
2046 UT. However, the important feature of these detailed data in the
magnetosphere- like region is that the field magnitude is extremely
steady and gives no indication that any of the variability of the
interplanetary magnetic field or the sheath region have been transmitted
into this region of the Hermean magnetosphere. This segment of
the data reflects what is ideally expected from observations obtained
while traversing any planetary obstacle on its darkside if the planet
possesses a magnetic field sufficiently strong to deflect the solar
wind and lead to the development of a detached bow shock wave.

Details from the outbound magnetopause and bow shock crossings are
shown in Figure 5. The magnetopause is identified at 2054 UT by the
abrupt change in the latitude angle θ from northward to southward. This
is followed by a period of relatively rapid alternating sign, seen
for approximately 40 sec. This is believed to reflect the relative
motion of the magnetopause and the variability of the magnetospheric
structure, probably due to variations in the interplanetary medium and

the response of the Hermean environment to these fluctuations. It may also reflect the close proximity of the spacecraft to a neutral sheet-field reversal region such as found in the earth's magnetic tail. The sheath region is again well defined by relatively larger amplitude fluctuations of all three field components.

With the better time resolution, the bow shock is now somewhat more distinctive. The fluctuations change from relatively lower frequencies and larger amplitudes to higher frequencies and smaller amplitudes. The period of bow shock crossings is extended however, from 2057 to 2059 UT, with a more distant bow shock crossing apparently observed just after 2100 UT.

The identification of the time occurrence of these various boundaries is important in determining the relative geometry of the positions of the solar wind obstacle boundary, the magnetopause, and the detached bow shock. The identified positions of the boundaries are superimposed on the trajectory plot of Figure 2 with uncertainties indicated accordingly. Also included are two curves representing a scaled magnetopause and bow shock, both obtained from theoretical studies of the solar wind interaction with the geomagnetic field. The shape of the magnetopause shown (14) is computed for the case of the solar wind incident upon a Hermean-centered magnetic dipole orthogonal to the solar wind flow (assumed along - X_{SE}) and the plane of the figure. The bow shock shown (15) is scaled according to a sonic Mach number of 10 and Alfvén Mach number of 20 at the subsolar point. These values correspond approximately to the measured values of the interplanetary magnetic field, plasma density and velocity. The theoretical bow shock position

presented here is for the only yet solvable case in magnetohydrodynamics, that of aligned flow, in which the upstream magnetic field and solar wind velocity are parallel. Since it is assumed that the apparent solar wind direction is parallel to the Mercury-Sun line, this implies a true flow from 3.7°E when taking into account the effect of aberration due to planetary heliocentric orbital motion.

No direct attempt has been made to adjust the scaled curves to exactly fit all observed boundary traversals. But the comparison with the observed boundary positions is remarkably good, considering the normal variability of the solar wind and its concomitant effects.

For this fit the value of the stagnation point distance (14)

$$r_{sp} = 1.07 \left[\frac{M^2}{4\pi mnV^2} \right]^{1/6}$$

has been assumed equal to 1.6 R_M (R_M = 2434 km). With the measured value of n = 17 p/cm^3 and the estimate of V $\approx$ 600 $\pm$ 50 km/sec, the magnetic moment M is determined to be 380 $\pm$ 32γ R_M^3.

ANALYSIS OF BOUNDARY CROSSINGS

The relative position of the bow shock and magnetopause boundaries is important in determining the geometry of the obstacle to solar wind flow. In order to obtain accurate estimates of the appropriateness of the fit of the bow shock and magnetopause boundaries, normal vectors to these surfaces have been calculated where possible. They are valuable since they augment the discrete point location by permitting extrapolation of the surface shape beyond the point of observation. This is analogous to a classical boundary value problem in which one has information which fixes the slope as well as the magnitude of a quantity of interest at

a specific boundary.

The inbound bow shock was first observed at 2027:20 UT, immediately followed by another crossing, which appears as a reverse shock, and finally the third and last crossing at 2027:50 UT. Average magnetic field quantities were used in estimating the shock normal. An analysis interval of 84 seconds immediately preceeding the first crossing and another interval of 84 seconds after the last crossing were used. Implicitly assumed is stationarity of the interplanetary magnetic field during 3-1/2 minutes. The pre- and post-shock field averages in standard XYZ solar ecliptic coordinates, normalized to unity, and their respective magnitudes were found to be

$$\hat{B}_{pre} = (0.630, -0.237, 0.740)$$

$$|\bar{B}|_{pre} = 17.3\gamma$$

and

$$\hat{B}_{post} = (0.497, -0.119, 0.860)$$

$$|\bar{B}|_{post} = 40.3\gamma$$

Hence, the field magnitude jump ratio was 2.3 and the angle between the pre- and post-field vectors was 12°, implying that the field vectors were almost parallel. Under this condition, calculation of the shock normal using the magnetic coplanarity theorem (16) is not applicable due to an unacceptable magnification of errors (17). Since data for the ion component of the plasma was not available, a more sophisticated method of least squares fitting to the shock conservation equations was not possible either (17).

However, it is obvious from the data that the shock character was

typically that of an approximately perpendicular type (i.e. the shock

surface normal is perpendicular to the upstream field). Thus, this was

assumed as was the cylindrical symmetry of the bow shock surface about

an axis parallel to the X-axis. With knowledge of the spacecraft

position at the crossing, this is sufficient to yield an accurate

estimate of the bow shock normal:

$$\hat{n}_{BS} = (0.65, \ 0.70, \ -0.30)$$

This corresponds to a longitude $\phi = 47^{\circ}$ and a latitude $\theta - 18^{\circ}$, while the

angle between the bow shock normal and the X-axis is 50°. The angle

between the projection of the bow shock normal onto the YZ plane and

the Y axis is found to be -23°. Figure 2 shows the bow shock normal

in terms of the relevant angles.

Using the upstream field magnitude of 17γ and the plasma density

of $n = 17$ particles/cm^{-3} from the Mariner 10 Plasma Science Experiment,

the upstream Alfvén speed is computed to be $V_A = 90$ km/sec. Assuming

that the protons behave according to the plasma bulk velocity-temperature

relationship valid at 1 A.U. (18), the sound speed is calculated to be

$V_s = 60$ km/sec. The component of the upstream plasma bulk speed along

the bow shock normal is 390 ± 32 km/sec, using the 600 ± 50 km/sec

value for the solar wind speed. Hence, the upstream fast mode Mach number

is 3.6 ± 0.3 and the sonic Mach number is 6.5 ± 0.5. This yields good

agreement with the magnitude of the field jump ratio of 2.3 (19).

The inbound crossing of the obstacle to solar wind flow was assumed

to be a classical MHD tangential discontinuity (16,20), across which no

plasma flow takes place and perpendicular to which no magnetic field

exists. Hence, using the magnetic field data alone, a normal to this
boundary, observed at 2036:50, was computed using 84 second averages
for pre- and post-observations. This yields a normal of

$$\hat{n}_{TD} = (0.30, \ 0.88, \ -0.36)$$

The angular coordinates of this normal are longitude $\phi = 72^{\circ}$ and latitude
$\theta = -21^{\circ}$. Accordingly, the angle with respect to the X axis is 73°
and to the Y axis in the YZ plane is -22°. The field magnitude jump
ratio across this boundary was 1.6. Such a tangential discontinuity
is expected at a classical magnetopause boundary crossing. It is often
the case for the terrestrial magnetopause.

A similar calculation has been done for the outbound crossing of
the obstacle boundary, which occurred at 2054:15 UT. The analysis
intervals chosen were 42 sec in order to obtain pre- and post-boundary
averages, while a 42 sec interval including the crossing was omitted due
to high RMS values of the components. From these data, the outbound
normal obtained is:

$$\hat{n}_{TD} = (0.26, \ -0.94, \ 0.21)$$

The longitude $\phi = 285^{\circ}$ and latitude $\theta = 13^{\circ}$. Accordingly the angle with
respect to the X axis is 75° and to the Y axis in the YZ plane is 13°. The
outbound tangential discontinuity normal is not as accurately determined
as in the case for the inbound crossing due to the greater fluctuations
of the magnetic field near the outbound obstacle boundary.

The outbound bow shock crossing occurring between 2057 and 2059 UT
and briefly at 2100 UT, appears to be a multiple crossing of a
pulsation shock. This occurs, as previously mentioned, when the shock
is a parallel type, i.e., when the field and shock normal are aligned
with each other (13).

Figure 2 includes the projection of the tangential discontinuity normals on the trajectory. In addition, the solid lines of Figure 2 correspond to theoretical boundary positions previously discussed. It is seen that there is remarkably good agreement with the normals so computed and the boundary positions calculated. This agreement of extrapolated surfaces determined from the normals computed at the boundary crossings and the boundary positions themselves leads us to conclude that the obstacle to solar wind flow is global in size. That is, it is not plausible to expect that a trailing shock such as a limb shock, due to the deflection of the solar wind near the terminators of the flow, would lead to the geometrical configuration and the shock strength measured by the Mach number which are required by these magnetic field data.

It should be noted that both the identification of the time of occurrence of these boundaries (bow shock and magnetopause) and the nature of their signature (abrupt or diffuse), is in excellent agreement with the Plasma Science Experiment on Mariner 10.

INTERPRETATION OF THE ORIGIN OF THE MAGNETIC FIELD

The origin of the interplanetary magnetic field upstream of either the bow shock or the magnetopause is the solar magnetic field. Within the magnetopause boundaries, the field is the vector sum of secondary magnetic fields associated with the solar wind interaction and any intrinsic planetary magnetic field.

There is no unique characteristic of the data itself which will permit separation of the internal and external contributions since the data is available only for a very restricted region of space, namely along the spacecraft trajectory. If the magnetic field data were available over a closed surface enclosing the planet, it would be possible to uniquely separate the internal and external sources using classical methods of mathematical analysis (21).

Thus, in our preliminary interpretation, we have considered the simple model of an offset, tilted dipole as representing the intrinsic field of the planet. Further, it is assumed that this represents the major contribution of the observed magnetic field only during the interval 2041-2050 UT, surrounding closest approach, when the spacecraft is within 2400 km of the planetary surface. Using selected data from this interval and by minimization of the mean-square fit of such an assumed dipole, we obtain a result whose fit to the data is illustrated in Figure 6. The three orthogonal magnetic field components, both observed and theoretical are presented and a reasonably good fit is obtained. Discrepancies, especially in the X component, can be explained as due to the secondary magnetic fields associated with currents flowing on the magnetopause extending the planetary magnetic field out behind the planet to form

a magnetic tail. While there are indications that the discrepancies after closest approach may be due to complex local fields on the planetary surface, most probably they represent time variations of the structure of the Hermean magnetosphere.

The coordinates and values of the dipole so determined are as follows:

Position: Offset = 0.47 R_m at $\phi = 62^o$ and $\theta = 17^o$

Moment: Magnitude = 227γ R_m^3 at $\phi = 209^o$ and $\theta = -70^o$

These preliminary values are uncertain, in a mathematical sense, by approximately 10% in offset distance, 20% in magnitude of dipole moment and 10° in all direction angles.

One characteristic of this intrinsic magnetic dipole is that it is oriented within 20° of the ecliptic pole or almost aligned with the axis of rotation of the planet, considering that there is an uncertainty of some 10° in the planetary rotation axis. The large offset might appear at first to be somewhat anomalous. However, with consideration of the very large core size (22) due to the anomalously high average density of the planet, it is quite acceptable.

A further implication of this dipole concerns the magnetic field configuration of the Hermean magnetosphere. The field on the surface of the planet is shown in the upper panel of Figure 7, in which an isointensity map of the intrinsic Hermean magnetic field is presented. Also included are intersections of the magnetic poles and equator and the trace of the Mariner 10 sub-spacecraft point. The field at an altitude of 0.6 planetary radii (1460 km elevation) is presented in the lower panel. This is the appropriate distance for the stagnation

point inferred in the previous section, when the interpretation of the
obstacle boundary and bow shock position was made.

Immediately evident in these two isointensity contour maps is the
asymmetry due to the dipole offset. The magnetosphere of Mercury is
clearly not as symmetrical about the Mercury-Sun line as the earth's
is about the earth-Sun line. However, it is plausible to assume that
a magnetic tail and embedded neutral sheet-field reversal region will
be developed on the darkside, similar to the earth's. Then the effect
of the dipole offset and tilt would be to bring the neutral sheet region
closer to the surface of the planet near the dawn terminator than at
the dusk terminator at the time of encounter, March 29, 1974. The
weaker fields and closer proximity to the magnetic equator, as Mariner 10
approached the outbound magnetopause, combine to yield a consistent
image of the origin of the field as due to an intrinsic but modest
magnetic field of the planet Mercury.

The offset of the dipole in the Y-Z plane will have an effect on
the positions of the magnetopause and bow shock. However, there is
some compensation due to the dipole tilt, so that the net effect may
not lead to a significant inconsistency with the results illustrated
in Figure 2 assuming a centered dipole with no tilt. Similarly, the
offset in the +X direction, 0.21 R_m, compensates the lower moment
determined, $227\gamma\ R_m^3$, relative to the value of $380\gamma\ R_m^3$ inferred only
from the boundary positions. The stagnation point distance from the
YZ plane is then found to be approximately 1.7 R_m, which compares
favorably with the previously used value of 1.6 R_m, considering the uncertainty
associated with the fitting of the theoretical bow shock and magnetopause

surfaces to the observed crossings and normals.

POSSIBILITIES OF INDUCTION MODE

The steady state or unipolar induction mode is generated by the $\vec{E} = -\vec{V} \times \vec{B}$ electrical field associated with the solar wind convective transport of the interplanetary magnetic field past the planet (23). The resulting electrical currents close in the solar wind, regardless if they are induced in the ionosphere or the planetary interior (24). Clearly then for such a mode there must be direct electrical contact between the ionosphere or planetary surface and the solar wind. Thus, the solar wind cannot be completely deflected away from the ionosphere or the planet itself.

The observations by Mariner 10 of the Hermean bow shock and magnetopause correspond to positions and characteristics which are not consistent with such a postulated geometry, wherein only a portion of the flow is deflected and this occurs very close to the planet. Also, the magnetic field topology as observed at the magnetopause traversals is not consistent with the theoretical field configurations in which the magnetic field is draped around the planet (24). A recent quantitative study of the steady state induction mode appropriate to the Moon assumes complete absorption of the solar wind on the upstream hemisphere (25). The magnetic field configuration obtained confirms the earlier qualitative studies (24) and does not show large directional changes of the magnetic field at what would correspond to the magnetopause, clearly seen in the Mariner 10 data. Finally, no modest sized magnetosphere-like region was observed at Venus (12), the normalized stagnation point distance being only 1.025 whereas at Mercury it is ≈ 1.6. These many considerations of boundary positions and inferred obstacle

size as well as solar wind deflection, existence of a magnetosphere-like

region, magnetic field topology and comparative solar interaction studies

lead us to conclude that the unipolar steady state induction mode was

not active at Mercury encounter.

The transient induction mode is generated by an implicit time

variation of the interplanetary magnetic field $\vec{B}$ as seen by the planet.

This can be due to either an explicit time variation of the interplanetary

magnetic field, $\frac{\partial \vec{B}}{\partial t}$, or a spatial variation, $\vec{V} \cdot \nabla \vec{B}$, due to the

convection past the planet of a spatially varying interplanetary field.

For this mode, electrical currents circulate completely within the

planetary ionosphere or interior and no direct electrical contact with

the solar wind is required. Again, the absence of a modest sized

magnetosphere at Venus during the extended period when such a feature

could have been observed suggests that even if a significant Hermean

ionosphere existed, the transient induction mode would not be active.

The quasi-static nature of the magnetic field observations during

the inbound portion of the Mariner 10 trajectory at Mercury encounter

is such that it implies that a magnetosphere-like region had existed for a

time scale at least on the order of the time interval from inbound bow

shock crossing to closest approach. This places a constraint on the

minimum conductivity of the planetary interior since the characteristic

time constant for decay of electrical currents in such a mode is given

by
$$\tau = \frac{\mu_0 \, \sigma \, R_m^2}{\pi^2}$$

Assuming a magnetic permeability of free space and a uniformly

conducting planet leads to a minimum conductivity of 10^{-4} mhos/meter.

This is not an unreasonable value for silicates at the elevated

temperatures which must be appropriate in the Hermean interior and is

easily satisfied by any metal phases although dependent very much upon

the detailed grain structure and intergrain electrical connections.

However, the value is rather implausible for near surface material even

at the subsolar point.

A uniformly conducting planet model is not a reasonable assumption

and in the case of an insulating shell surrounding a conducting core, it

is clear that a combination of higher magnetic permeability and conductivity

is required. Neither of these two requirements creates special problems

for Mercury because its high average density implies a substantial iron

rich core (22). Moreover, the secondary magnetic field which would

develop in such a mode is dominated by a dipole term. Since there were

significant, abrupt changes in the interplanetary magnetic field direction

near 2020 UT, we do not believe it possible at present to reject this

induction mode possibility. However, it requires a unique combination

of circumstances coincident with the time of encounter and also a very

strong secondary field, much stronger than in the lunar case, in order

that the obstacle be as large as has been inferred. We believe the

most plausible explanation is the conclusion offered in the previous

section that there exists a modest intrinsic magnetic field

of Mercury.

DISCUSSION

In the previous sections, arguments for the interpretation of the

magnetic field observations in terms of a modest intrinsic planetary

magnetic field have been presented. The analysis yielding an offset,

tilted dipole explicitly assumed that there were no time variations in the structure of the Hermean magnetosphere during Mariner 10 observations. However, it should be noted that the characteristic change in magnetic field data from a tail-like configuration to a more dipolar-like configuration following closest approach may be due to a temporal change in the Hermean magnetospheric structure. By intercomparison of these data with the plasma and particle measurements, it should be possible to clarify this possibility.

One effect of such a temporal variation on the interpretation would be that it could masquerade as a spatial variation of the magnetic field and lead to an erroneous conclusion regarding the magnitude of the dipole offset and tilt.

The implication of these results regarding the present state and past history of formation of the planet Mercury is significant. The presence of an intrinsic planetary magnetic field may be due to a dynamo currently active within the planetary interior or a residual remanent magnetic field associated with a now extinct dynamo. Thus, it is possible that the planet Mercury rotated faster earlier in its history than is presently observed. On the other hand if the transient induction mode is the source of the field, it places a constraint on the interior electrical conductivity.

Assuming that the intrinsic dipole interpretation is correct, then significant conclusions regarding the solar wind interaction with Mercury in its present state can be reached. The large offset and modest size of the dipole moment suggest that under normal conditions Mercury should not possess a persistent permanent trapped radiation belt. However, a

magnetic tail should exist and contain within it an embedded neutral sheet-field reversal region where particles are accelerated by field line merging.

Because the dipole is approximately perpendicular to the planet's orbital plane, the size of the Hermean magnetosphere and tail would not change significantly during the Hermean year. However, the distance of the stagnation point of solar wind flow relative to the subsolar point on the planetary surface will change considerably because of the large dipole offset. Due to the variation in heliocentric distance of Mercury and temporal variations in the solar wind momentum flux and the changing value of the planetary field in the subsolar region, it will be possible for the solar wind to compress the planetary field to the surface. Thus, since the surface of the planet will not always be protected from the direct impact of solar wind flux, the optical properties of the planet surface in certain regions should reflect the effects of proton bombardment characteristically observed on the lunar surface.

If Mercury also has a weak atmosphere, then acceleration of particles in the neutral sheet might lead to precipitation of particles into the polar regions and to "auroral" events. Direct access of particles from the interplanetary medium to the polar region is always possible.

These are speculative remarks, but represent logical conclusions reached from the existence of an intrinsic Hermean magnetic field. We once again emphasize the preliminary nature of the interpretation. The offset, tilted dipole result inferred in this first analysis should not be taken as more than a logical and simplified starting point for studying what is most certainly a complex interactive process. We

interpret these results, however, as being highly suggestive that an intrinsic field does indeed exist. Final confirmation of this conclusion will be possible if another appropriately configured Mercury encounter takes place. Unfortunately, the second encounter by Mariner 10 will not satisfy this requirement and it is not expected therefore to contribute any additional useful data to these investigations.

CONCLUSIONS

Direct observations of the magnetic field environment of Mercury by the GSFC Magnetic Field Experiment on Mariner 10 show the presence of a well developed bow shock wave and magnetosphere region. A fundamental question not yet uniquely resolved is whether or not the magnetic field observations are consistent with an intrinsic planetary magnetic field or one induced by solar wind interaction. Considering the well studied case of solar wind interaction with the Moon and the recent Mariner 10 observations at Venus, it appears that the magnetic field data are not consistent with the steady state induction mode of interaction but may be consistent with the transient mode.

The modest size of the apparent magnetosphere of Mercury precludes a determination of an assumed intrinsic magnetic moment with high confidence. Using a restricted data set near closest approach, preliminary analysis yields an offset tilted dipole whose parameters are generally consistent with other aspects of the data. The moment's magnitude is $227\gamma\ R_m^3$, which is 5.5×10^{-4} that of the earth's dipole moment. Whereas the dipole's offset is significant, $0.47\ R_m$, the tilt is within 20° of the ecliptic pole. This is probably close to the planetary rotation axis, itself uncertain to 10°. With the anomalously high average density of this small terrestrial planet, such a large dipole offset is not implausible.

It should be noted however, that temporal variations of the structure

of the magnetosphere of Mercury would masquerade as spatial variations

of the magnetic field in the interpretation of data from a single flyby

encounter.

If the interpretation of an intrinsic planetary magnetic field

at Mercury is validated by future studies and additional observations,

it will represent a substantial discovery in the exploration of the

solar system and contribute significantly to the study of its origin.

Figure Captions

Figure 1   Four models of the solar wind interaction with a
                planetary sized object. The weakest interaction mode,
                A, is typified by the Moon and occurs in the case of
                an insufficient intrinsic magnetic field or atmosphere/
                ionosphere to deflect the solar wind. In all other
                models, a bow shock develops because of the deflection
                of   super Alfvénic flow around the planet, due to a
                sufficient atmosphere/ionosphere in model B; a sufficiently
                conducting planetary interior in model C or a sufficient
                intrinsic planetary magnetic field as in the case of
                the earth, in model D.

Figure 2   Encounter trajectory of Mariner 10 in Hermean
                centered solar ecliptic coordinates (+ X_{SE} axis towards
                sun, Z_{SE} axis perpendicular to ecliptic, and Y_{SE} axis
                completing right handed coordinate system). The left
                hand panel presents a plot of the distance from the
                X_{SE} axis as ordinate while the right hand panel presents
                a true projection of the trajectory as viewed from the
                Sun.

Figure 3   GSFC 6 second averaged magnetic field data during
                Mercury encounter in spacecraft centered solar ecliptic
                coordinates. The latitude of the magnetic field vector
                is represented by θ and the longitude by ϕ. RMS represents
                the pythagorean mean of the X, Y, Z component root mean
                square deviations computed during the 6 second period.

Significant discontinuities observed in the magnetic field data are identified.

Figure 4   GSFC detailed magnetic field data with instrument sampling rate of 25 Hz during inbound bow shock and magnetopause crossings and near closest approach (CA). The three orthogonal components are presented in the bottom three traces.

Figure 5   GSFC detailed magnetic field data during the outbound magnetopause and bow shock crossings.

Figure 6   Comparison of 6 second averaged observations of the three orthogonal components of the magnetic field near closest approach with a theoretical planetary magnetic field. It is represented by an offset, tilted dipole chosen to best fit the data in a least squares measure during the interval 2041-2050 UT. (See text).

Figure 7   Predicted isointensity contours and characteristics of intrinsic magnetic field on Hermean surface (upper panel) and at 1460 km elevation from surface (lower panel). The polarity of the magnetic poles is in the same sense as Earth's. The appreciable offset distorts the surface field so that there is more than an order of magnitude variation over the surface. The position of Mariner 10 during encounter trajectory and the associated bow shock and magnetopause crossings are indicated relative to the magnetic equator.
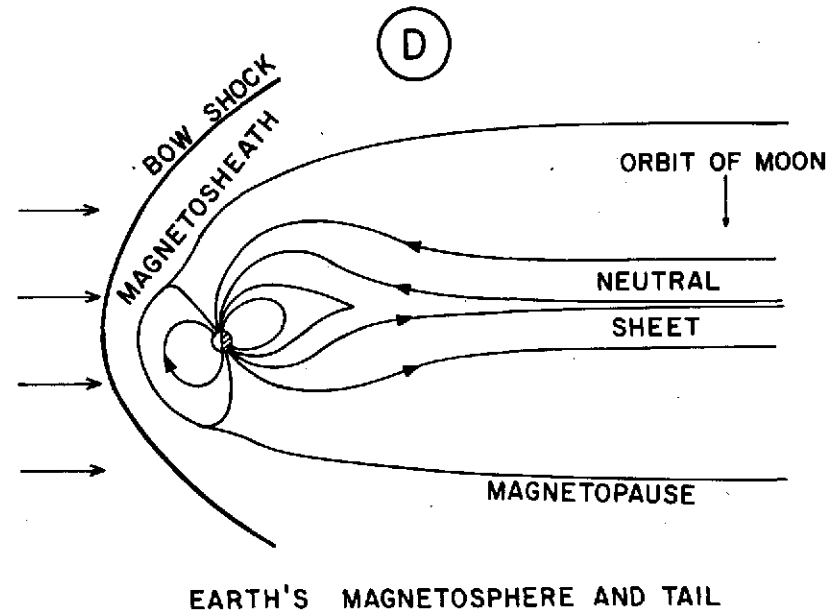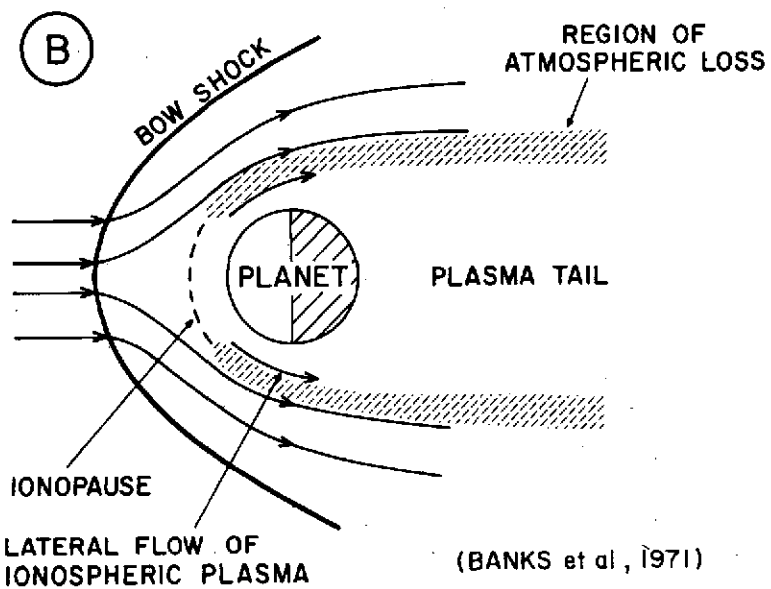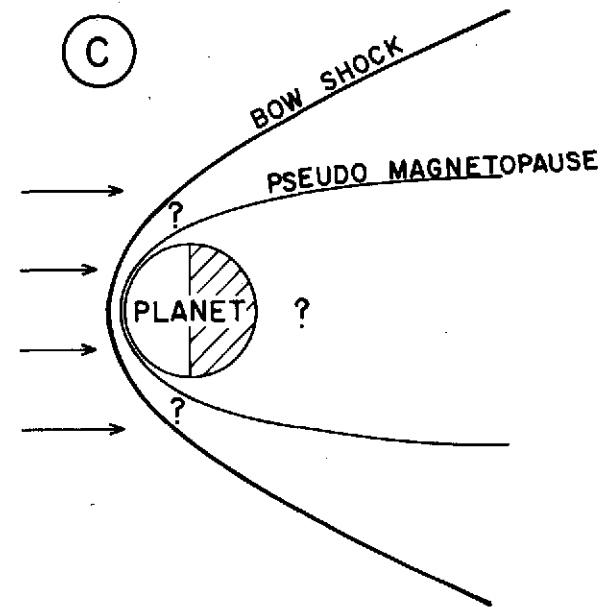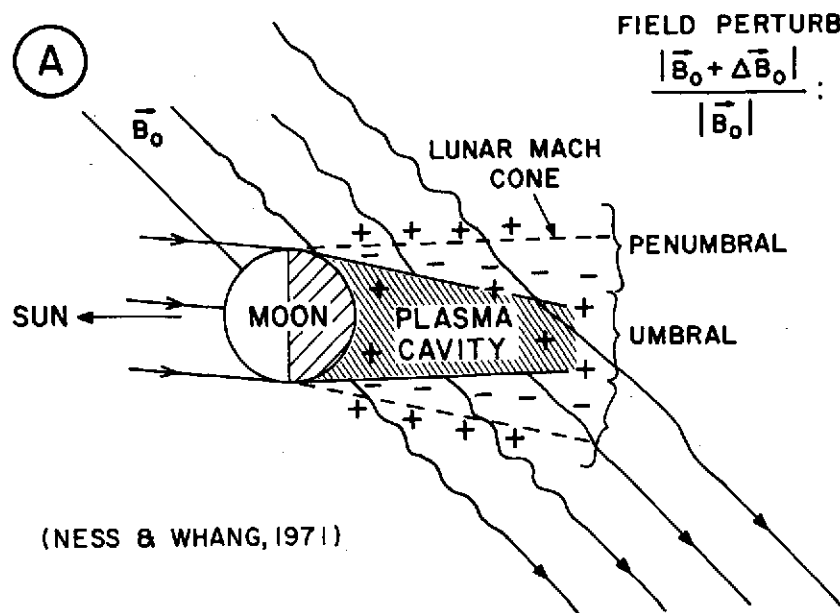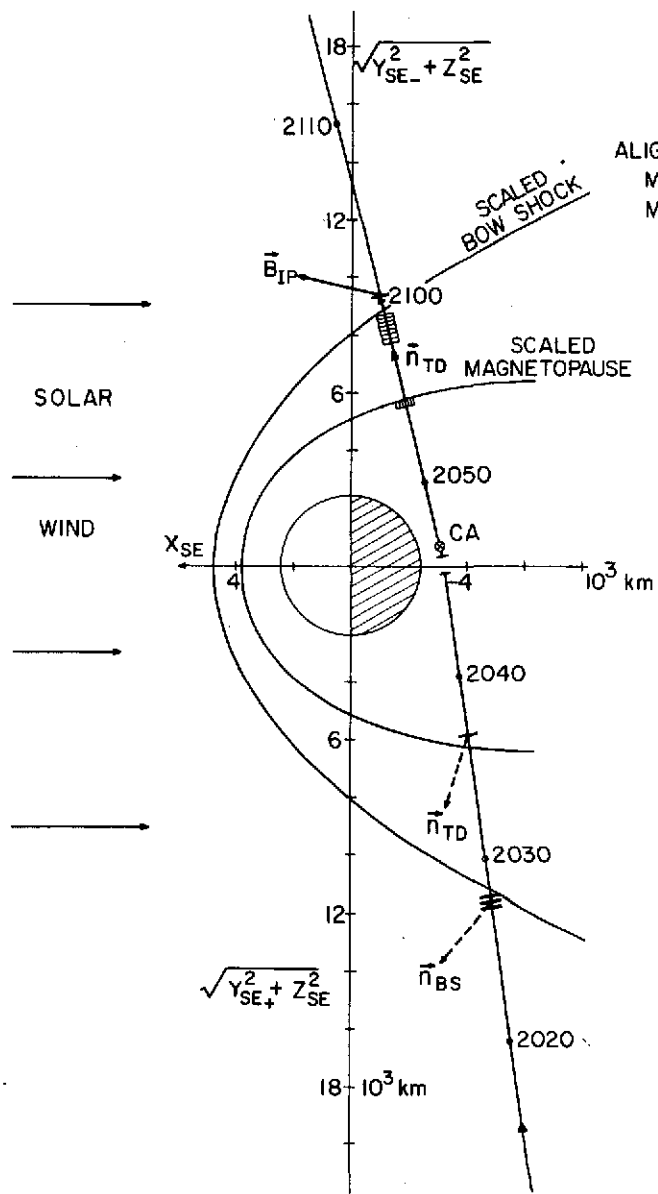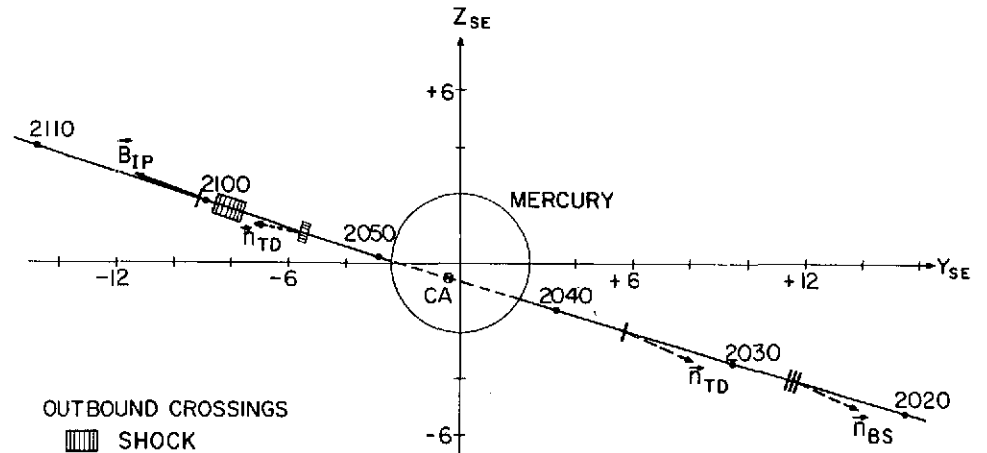
A

FIELD PERTURBATIONS:

$$\frac{|\vec{B_0} + \Delta\vec{B_0}|}{|\vec{B_0}|} : \begin{matrix} > 1 & + \\ < 1 & - \end{matrix}$$

$\vec{B_0}$

LUNAR MACH CONE

PENUMBRAL

SUN

MOON

PLASMA CAVITY

UMBRAL

(NESS & WHANG, 1971)

C

BOW SHOCK

PSEUDO MAGNETOPAUSE

PLANET

?

B

BOW SHOCK

REGION OF ATMOSPHERIC LOSS

PLANET

PLASMA TAIL

IONOPAUSE

LATERAL FLOW OF IONOSPHERIC PLASMA

(BANKS et al , 1971)

D

BOW SHOCK

MAGNETOSHEATH

ORBIT OF MOON

NEUTRAL

SHEET

PLANET

MAGNETOPAUSE

EARTH'S MAGNETOSPHERE AND TAIL

-29-

Figure 1

Figure 2

Figure 3

Figure 4

29 MARCH 1974
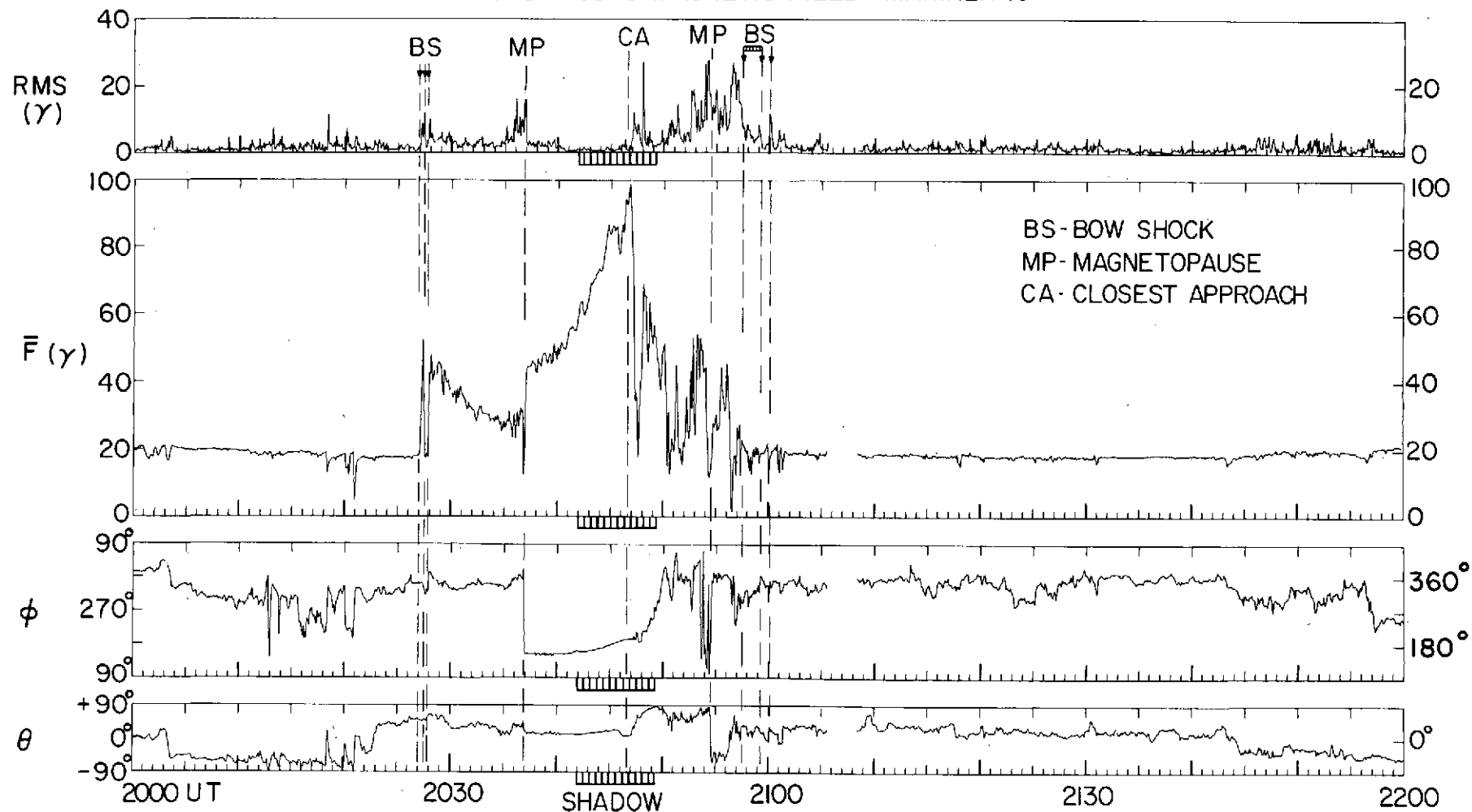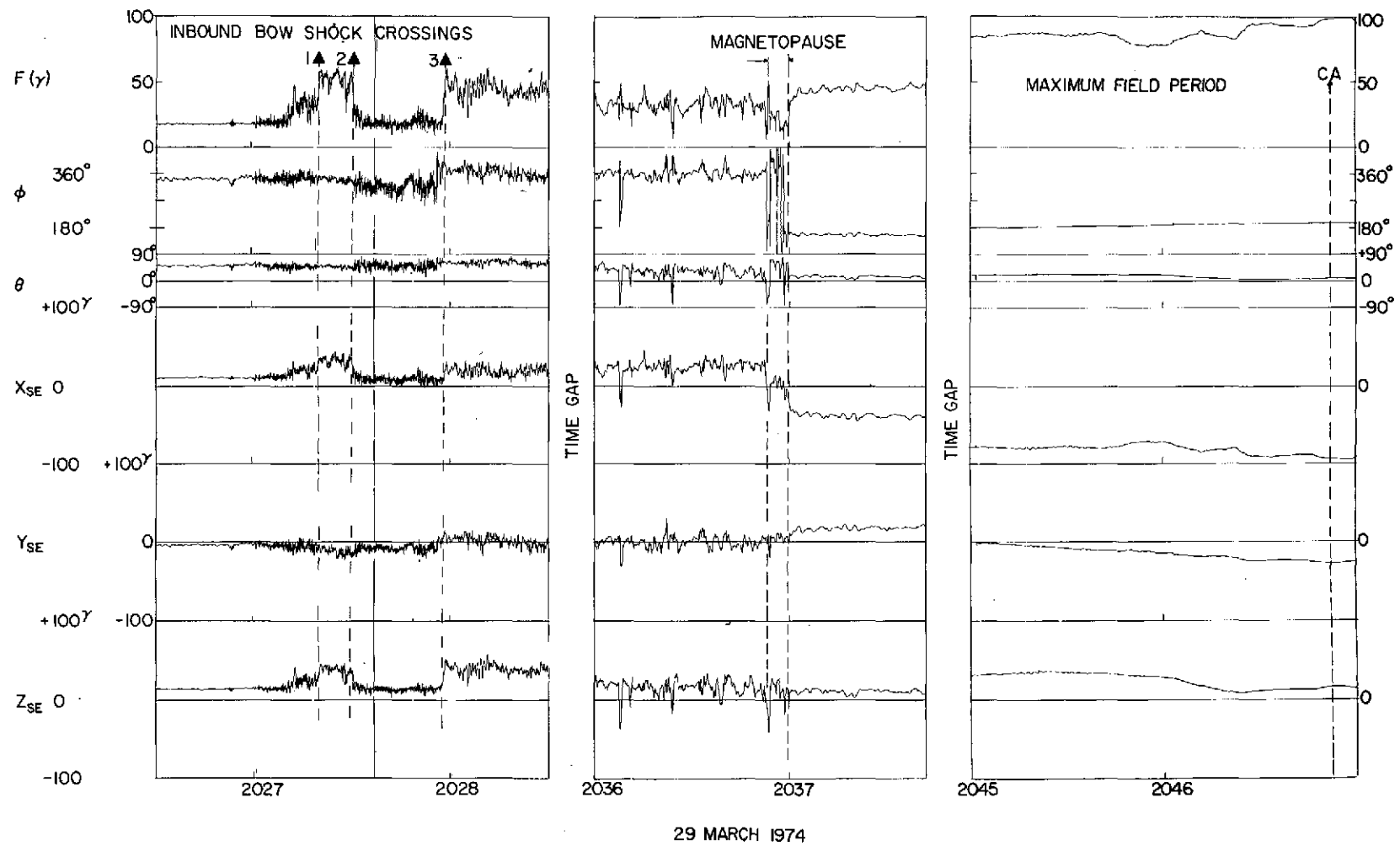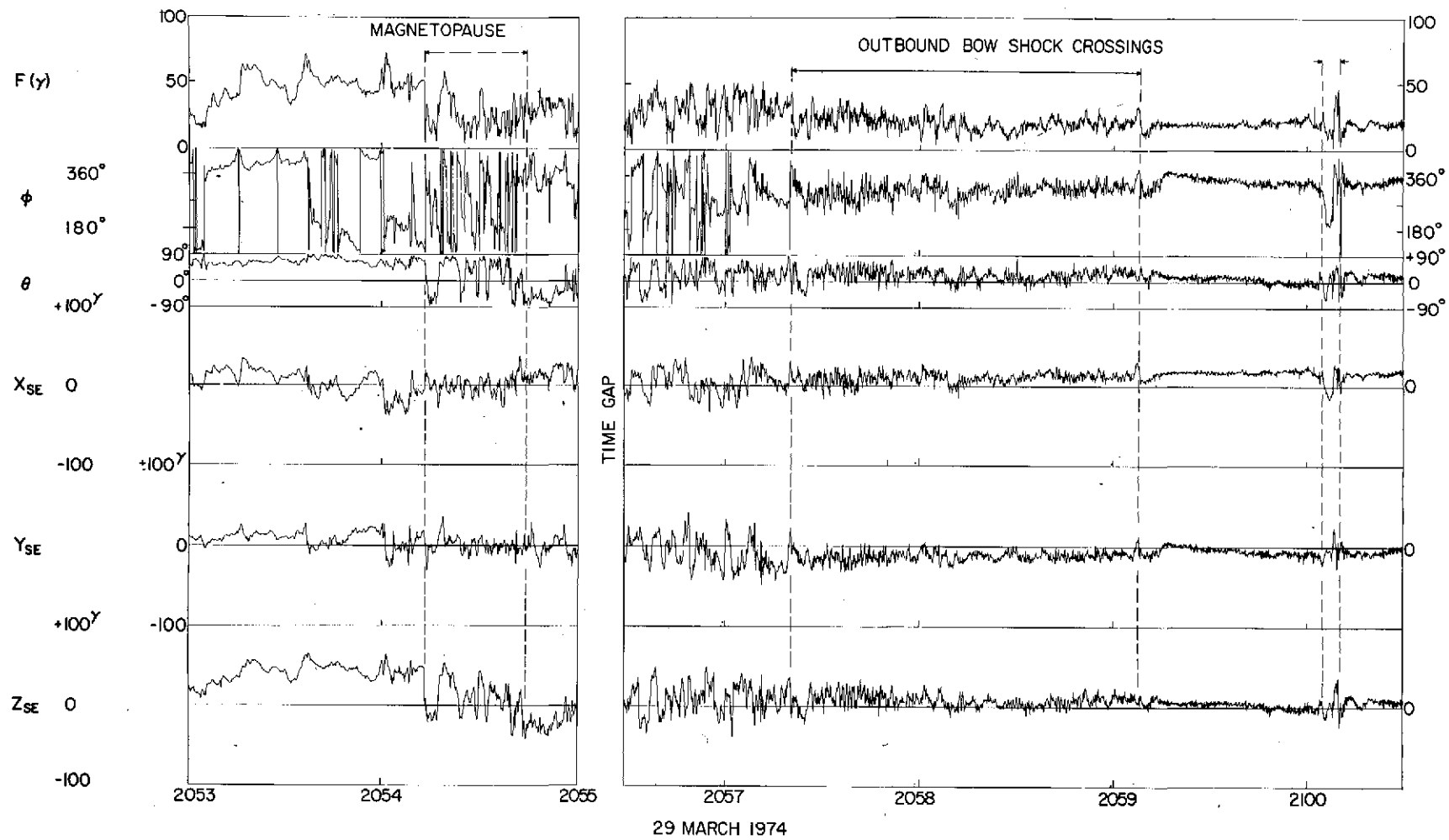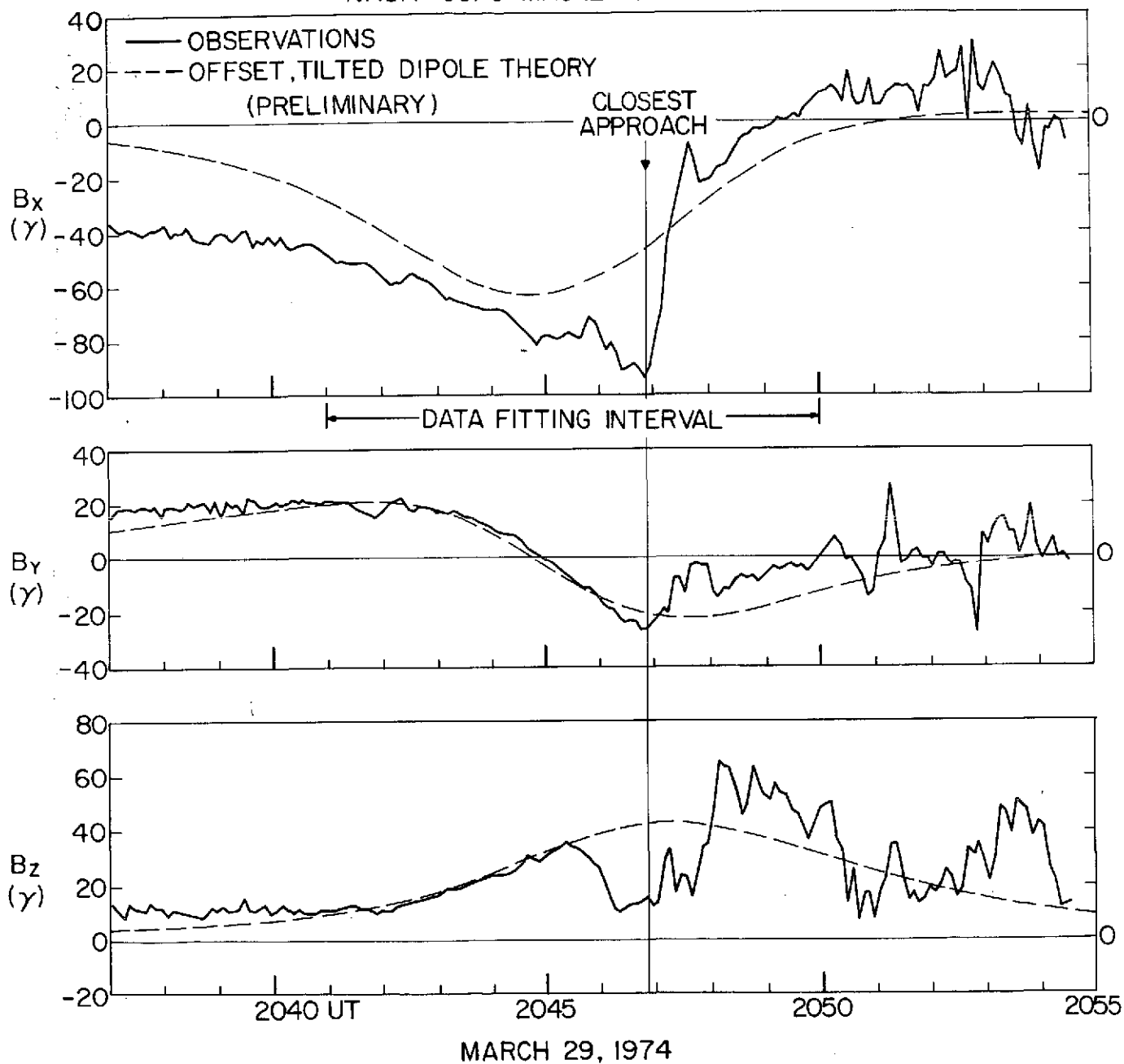
Figure 5

Figure 6

INTENSITY OF MERCURY'S INTRINSIC MAGNETIC FIELD ON SURFACE
(PRELIMINARY OFFSET, TILTED DIPOLE)

NOON
MERIDIAN
29 MARCH 1974
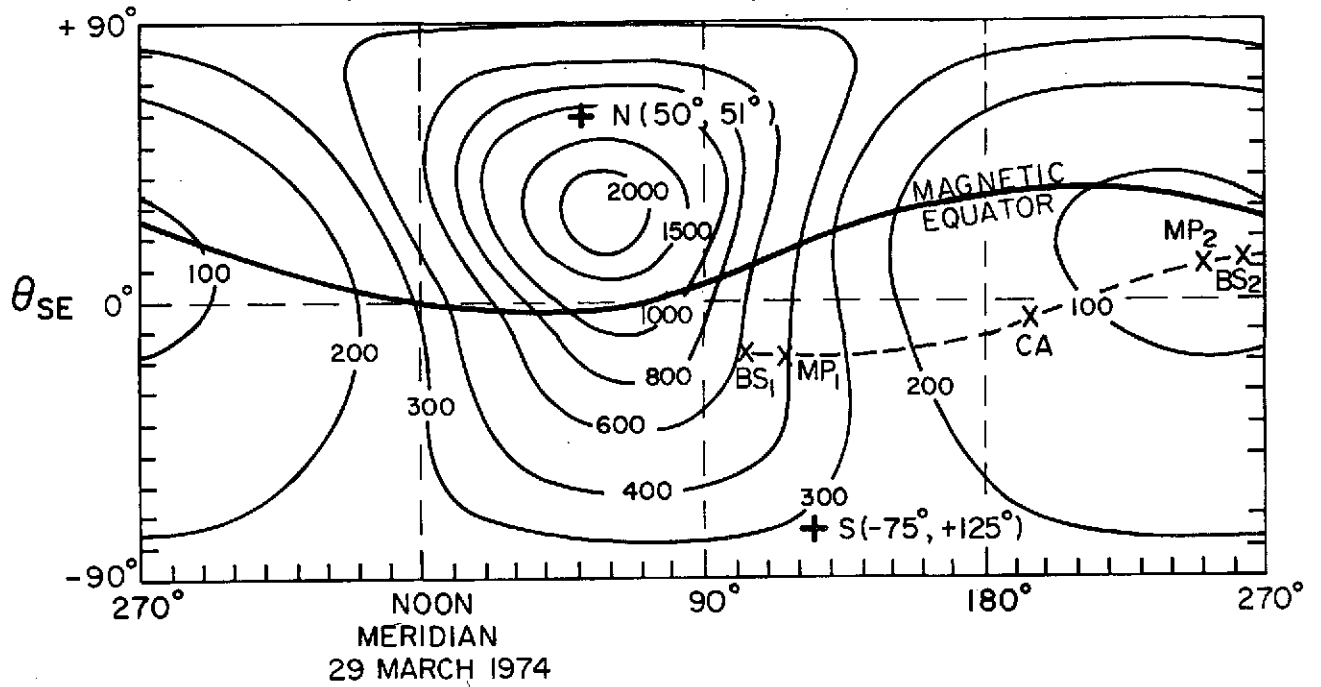
INTENSITY EXTRAPOLATED TO 1.6 R_M (1460 Km ABOVE SURFACE)
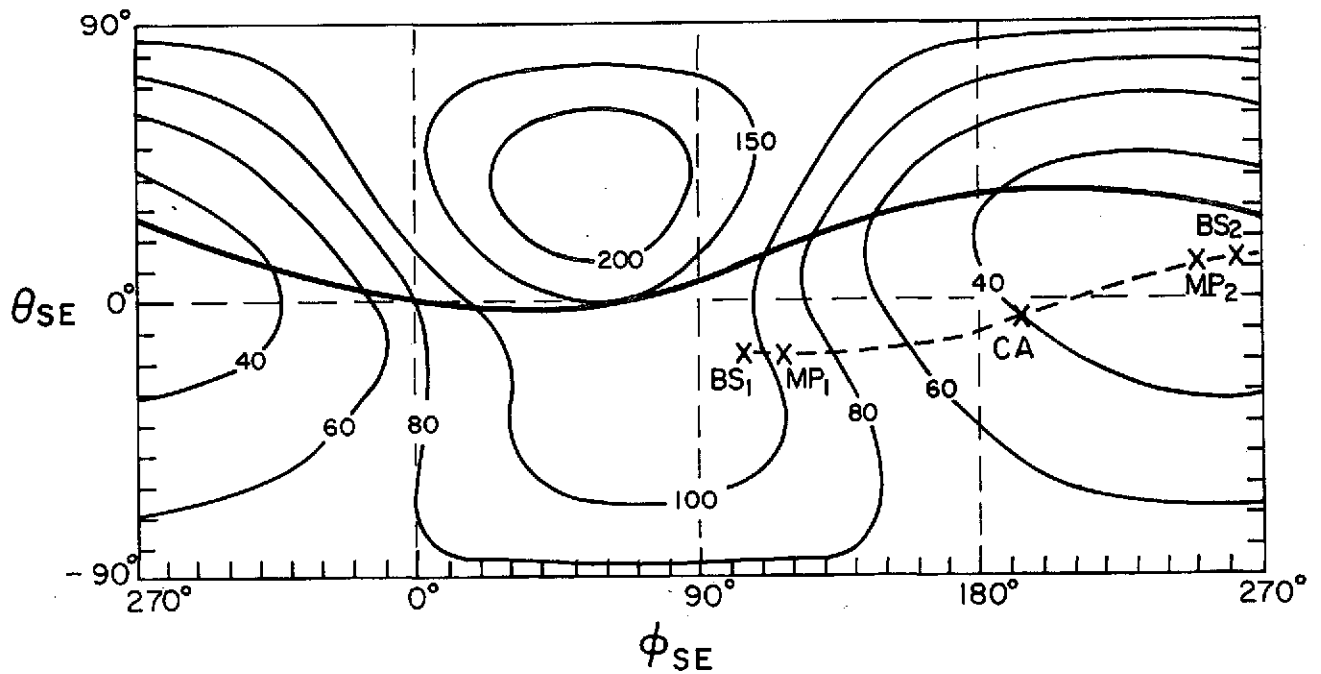

Figure 7

REFERENCES

1. C. H. Pettingill and R. B. Dyce, Nature 206, 1240 (1965).

2. G. Columbo, Nature 208, 575 (1965); P. Goldreich and S. Peale,
    Astron. J. 71, 425 (1966); G. Columbo and I. I. Shapiro, Astrophy. J.,
    145, 296 (1966).

3. G. P. Kuiper, Comm. Lunar Planet. Lab. 143, 169 (1970).

4. S. J. Peale, Icarus 17, 168 (1972); S. J. Peale, Astron. J. (to
    appear) 1974.

5. G. Field, in The Origin and Evolution of the Atmospheres and Oceans
    edited by P. J. Brancazio and A. G. W. Cameron, N.Y., J. Wiley and
    Sons (1964).

6. S. I. Rasool, S. H. Gross and W. E. Mc Govern, Space Sci. Revs. 5,
    565 (1966).

7. D. Morrison and C. Sagan, Astrophys. J. 150, 1105 (1967); D. Morrison
    Space Sci. Revs. 11, 271 (1970).

8. W. Elsasser, Phys. Rev. 64, 1946; E. C. Bullard and H. Gellman,
    Phil Trans. Roy. Soc. (London) Ser. A, 247, 213 (1954);
    W. V. R. Malkus, Science 160, 259 (1968); D. Gubbins, Revs. Geophys.
    Space Physics 12, 137 (1974).

9. N. F. Ness and Y. C. Whang, J. Geophys. Res. 76, 3136 (1971).

10. P. M. Banks, H. E. Johnson and W. I. Axford, Comments on Astrophys.
    and Space Physics 4, 214 (1970).

N. F. Ness
K. W. Behannon
R. P. Lepping
NASA-Goddard Space Flight Center
Greenbelt, Maryland 20771

Y. C. Whang
Catholic University of America
Washington, D. C.

K. H. Schatten
Victoria University
Wellington, New Zealand

11. C. P. Sonett and D. S. Colburn, Phys. Earth Planet. Interiors 1, 326 (1968); J. L. Blank and W. Sill, J. Geophys. Res. 74, 736 (1969); G. Schubert and K. Schwartz, The Moon 1, 106 (1969).

12. N. F. Ness, K. W. Behannon, R. P. Lepping, Y. C. Whang and K. H. Schatten, Science 183, 1301 (1974).

13. E. W. Greenstadt, I. M. Green, G. T. Inouye, D. S. Colburn, J. H. Binsack and E. F. Lyon, Cosmic Elec., 1, 160, 279 and 316 (1970); E. W. Greenstadt, J. Geophys. Res. 77, 1729 (1972), 5467 (1972); T. G. Northrop, T. J. Birmingham, ibid 78, 2308 (1973).

14. J. Y. Choe, D. B. Beard and E. C. Sullivan, Planet. Space Sci. 21, 485 (1973).

15. A. W. Rizzi, Ph.D. Thesis, Stanford University (1971).

16. D. C. Colburn and C. P. Sonett, Space Sci. Revs. 5, 439 (1966).

17. J. K. Chao, MIT Report CSR TR-70-3 (1970); R. P. Lepping and P. D. Argentiero, J. Geophys. Res. 76, 4349 (1971).

18. L. F. Burlaga and K. W. Ogilvie, Astrophys. J. 159, 659 (1970).

19. G. R. Smit, ESRO Report SN-17, ESRIN (1967); B. Bavassano, F. Mariani, U. Villante and N. F. Ness, J. Geophys. Res. 76, 5970 (1971); 77, 2004 (1972).

20. L. F. Burlaga and N. F. Ness, Solar Phys. 9, 467 (1969); D. M. Willis, Revs. Geophys. Space Phys. 9, 953 (1971).

21. S. Chapman and J. Bartels, Geomagnetism, Clarendon Press, Oxford, (1940).

22. S. Plagemann, J. Geophys. Res. 70, 985 (1965); R. A. Lyttleton, Astrophys. and Space Sci. 5, 18 (1969).

23. D. S. Colburn, C. P. Sonett and K. Schwartz, Earth and Planet. Sci. Letters, 14, 325 (1972).

24. A. J. Dessler, in Atom. of Venus and Mars, ed. by J. C. Brandt and M. B. McElroy, Gordon and Breach, N. Y., p.241 (1968); F. S. Johnson and J. E. Midgeley, Space Research, 9, 760 (1969); F. C. Michel, Revs. Geophys. Space Sci., 9, 427 (1971); J. L. Blank and W. R. Sill, Bellcom TM 72-2015-1 (1972); P. A. Cloutier and R. E. Daniell, Planet. Space Sci., 21, 463 (1973).

25. B. Horning and G. Schubert, J. Geophys. Res. 79 (to appear) 1974.